MYCOLOGIA
2025, VOL. 117, NO. 6, 1077–1087
https://doi.org/10.1080/00275514.2025.2544251

Taylor & Francis
Taylor & Francis Group

Epitypification of *Armillaria solidipes*, a cause of Armillaria root disease in North America

Vladimír Antonín[a], Ada J. Fitz Axen[b], Jorge R. Ibarra Caballero[b], James J. Worrall[c], Suzanne B. Marchetti[c], Jane E. Stewart[b], Ned B. Klopfenstein[d], and Mee-Sook Kim[e]

[a]Department of Botany, Moravian Museum, Zelný trh 6, Brno 659 37, Czech Republic; [b]Department of Agricultural Biology, Colorado State University, 307 University Avenue, Ft. Collins, Colorado 80523; [c]Rocky Mountain Region Gunnison, United States Department of Agriculture, Forest Service, Gunnison, Colorado 81230; [d]Rocky Mountain Research Station, United States Department of Agriculture, Forest Service, 1221 South Main Street, Moscow, Idaho 83843; [e]Pacific Northwest Research Station, United States Department of Agriculture, Forest Service, 3200 SW Jefferson Way, Corvallis, Oregon 97331

ABSTRACT

Although *Armillaria solidipes* was described in 1900, confusion has surrounded the appropriate use of this taxonomic epithet, largely because DNA sequence–based characterization and an associated culture were unavailable for the original holotype. An epitype for *A. solidipes* (previously known as North American Biological Species I) is established herein, along with morphological descriptions and genetic characterization that clearly distinguish *A. solidipes*, which is found in North America, from *A. ostoyae* (previously known as European Biological Species C), which is found in Eurasia. Of the five loci examined, translation elongation factor 1-alpha was the most useful for distinguishing *A. solidipes* from other *Armillaria* spp. including *A. ostoyae*. Further, the whole genome phylogeny of *A. solidipes* and *A. ostoyae* showed substantial differences that further demonstrate their separation. The specimen from Colorado, USA, which was collected in the locality where the original type specimen was collected, is designated as the epitype.

ARTICLE HISTORY
Received 10 March 2025
Accepted 2 August 2025

KEYWORDS
Armillaria ostoyae; epitype; Physalacriaceae; taxonomy; *tef1*; vicariance

INTRODUCTION

Armillaria solidipes Peck was described from a specimen collected in Colorado, USA (Peck 1900). However, precise characterization of the type specimen remained elusive. The type specimen was located in the Farlow Herbarium by Baroni (1981), who published the type revision without any taxonomic conclusion. Following the biological species concept, an interfertility test developed by Hintikka (1973) was used to define biological species of *Armillaria* in Europe and North America (Anderson and Ullrich 1979; Korhonen 1978). Interfertility testing determined that North American Biological Species (NABS) I was interfertile with European Biological Species (EBS) C (Anderson et al. 1980). Subsequently, EBS C was called *A. ostoyae* (Romagn.) Herink (Herink 1973; Romagnesi 1970) or *A. obscura* (Schaeff.) Herink; however, *A. ostoyae* (Romagn.) Herink (Herink 1973; Romagnesi 1970) was determined to be the appropriate name based on the availability of a type specimen, and *A. ostoyae* was also previously considered to be the appropriate name for NABS I (Burdsall and Volk 1993; Marxmüller 1992).

Following the results of the type revision, Burdsall and Volk (2008) synonymized *A. solidipes* with *A. ostoyae* and considered *A. solidipes* to be correct name for the latter species; however, these authors also conceded that *A. ostoyae* could be used for the European taxon should further research determine that it is distinct from the North American taxon. Later, Redhead et al. (2011) proposed to conserve *A. ostoyae* against *A. solidipes*; this proposal was later approved (Wilson 2017).

Uncertainty has continued about which *Armillaria* specimens or isolates are appropriately comprised in *A. solidipes*, largely because no DNA sequence information was obtained from the original holotype of *A. solidipes* (Burdsall and Volk 2008). Previous efforts to amplify rDNA from the original *A. solidipes* holotype were unsuccessful—perhaps due to degraded DNA or chemical contamination (H. H. Burdsall Jr., personal communication). In subsequent years, *Armillaria* taxonomy has been based on phylogenetic species concepts (Heinzelmann et al. 2019). Multiple phylogenetic and phylogenomic studies have shown that *A. solidipes* (formerly referred to as North American *A. ostoyae*) is clearly distinct from *A. ostoyae* from Eurasia (Guo et al. 2016; Ibarra Caballero et al. 2023; Klopfenstein et al. 2017; Liang et al. 2021). Based on a multilocus

CONTACT Vladimír Antonín vantonin@mzm.cz; Mee-Sook Kim meesook.kim@usda.gov
Supplemental data for this article can be accessed online at https://doi.org/10.1080/00275514.2025.2544251.

Published online 24 Sep 2025

phylogeny, Guo et al. (2016) provisionally assigned *A. solidipes* to isolates from North America and *A. ostoyae* to isolates from Eurasia. Furthermore, phylogenetic analyses show that North American *A. solidipes* is a sister taxon to *A. gemina* Bérubé & Dessur. in the Solidipes/Ostoyae superclade (Coetzee et al. 2018; Guo et al. 2016; Klopfenstein et al. 2017; Koch et al. 2017).

The aim of this study is to characterize *A. solidipes* in terms of morphology and assess its phylogenetic relationships with known North American and European taxa, while also establishing an *A. solidipes* epitype accompanied by an ex-epitype (cultured isolate) and whole genome sequence, which will allow continued characterization of *A. solidipes*.

MATERIALS AND METHODS

Isolates/specimens and culture.—In 2018, two connected basidiomata of this species were collected in the type locality of Mill Creek, near Gunnison, Colorado, USA, in the vicinity where the original holotype of *A. solidipes* was collected by Peck (1900) (FIG. 1). A culture was established from a small piece of internal tissue taken from the upper stipe of the largest basidioma that was transferred to malt extract agar (MEA) medium (3% malt extract, 3% dextrose, 1% peptone, 1.5% agar). This material was studied, and both basidiomata were selected as epitype of *A. solidipes*, with the accompanying basidoma-derived culture serving as the ex-epitype. The epitype of *A. solidipes* and other *Armillaria* isolates, species, cultures, and GenBank accession numbers used for the phylogenetic analyses are listed in TABLES 1 and 2. The epitype specimen has been deposited in the herbarium of the Department of Botany, Moravian Museum, Czech Republic, under accession number BRNM 847568. And the ex-epitype culture (GN1) has been deposited into the American Type Culture Collection (ATCC) as accession number 2024-TSDA-00053.

Morphology.—The macroscopic description is based on fresh basidiomata collected in Colorado, USA, and color descriptions followed Kornerup and Wanscher (1983). The microscopic description is based on dry basidiomata. Sections were mounted in KOH, Melzer's reagent, and Congo red and observed using an Olympus BX50 light microscope (Tokyo, Japan) with a magnification of 1000×. For basidiospores, the factors E (quotient of length and width in any one spore) and Q (mean of E-values) were used. The notation [a/b/c] at the beginning of description microscopic structures means "a" structures were measured from "b" basidiomata taken from "c" collections. Herbarium abbreviations follow Thiers (continuously updated).

Figure 1. *Armillaria solidipes* basidiomata collected by S. B. Marchetti and J. J. Worrall on *Picea engelmannii* in 2018 near Gunnison, Colorado, USA, in the vicinity where the original holotype of *A. solidipes* was collected by Peck (1900). Both basidiomata serve as the epitype BRNM 847568.

DNA extraction and sequencing.—For DNA extraction, mycelial tissues (ca. 50–100 mg) of selected *Armillaria* isolates (GN1, ST1, ST2, P1404, R1, R8, ST8, ST9, ST11, OHIO_2018 PB-1, and OOI-210) were scraped directly from 0.22-µm-pore MF-Millipore Membrane nylon filters (MilliporeSigma, Burlington, Massachusetts) overlaying a culture medium to support mycelial growth (TABLE 1) (Antonín et al. 2021). DNA extraction was conducted according to the ZR Fungal/Bacterial DNA MiniPrep Kit protocols supplied by Zymo Research (Irvine, California). DNA concentration was measured using a NanoDrop 2000 spectrophotometer (Thermo Fisher Scientific, Waltham, Massachusetts). Following the methods of Antonín et al. (2021), polymerase chain reaction (PCR) was used to amplify the following five loci for sequencing: translation elongation factor 1-alpha (*tef1*), RNA polymerase II second largest subunit (*rpb2*), glyceraldehyde-3-phosphate dehydrogenase (*gpd*), actin

Table 1. List of *Armillaria* species, isolates, and GenBank accession numbers used for this study.

			GenBank accession numbers[a]				
Isolate	Species	Country/Origin	*tef1*[b]	*act*	28S	*gpd*	*rpb2*
GN1[c]	*Armillaria solidipes*	USA: Colorado	*PP481735*	*PP481930*	*PP342531*	*PP484600*	*PP501799*
ST1	*A. solidipes*	USA: New Hampshire	JF313141	*PP481935*	AY973657	*PP484604*	*PP501804*
ST2	*A. solidipes*	USA: Washington	JF313139	*PP481936*	AY973728	*PP484605*	*PP501805*
P1404	*A. solidipes*	USA: Idaho	JF313140	*PP481932*	AY973682	*PP484601*	*PP501801*
V91-02	*A. solidipes* (as *A. ostoyae*)	Canada	FJ618667	FJ618623	FJ618754	FJ618710	FJ618798
JB13	*A. solidipes* (as *A. ostoyae*)	Canada	FJ618637	FJ618592	FJ618723	FJ618680	FJ618768
R1	*A. solidipes*	USA: Idaho	*PP481736*	*PP481933*	*PP342533*	*PP484602*	*PP501802*
R8	*A. solidipes*	USA: North Carolina	*PP481737*	*PP481934*	*PP342534*	*PP484603*	*PP501803*
PC88.22	*A. ostoyae*	Italy	HQ891859	FJ618634	FJ618765	FJ618715	FJ618803
PC82.4	*A. ostoyae*	Germany	FJ618656	FJ618611	FJ618742	FJ618698	FJ618786
PJC94.5	*A. ostoyae*	South Korea	FJ618653	FJ618608	FJ618739	FJ618696	FJ618784
PA87-82	*A. borealis*	Russia	FJ618642	FJ618597	FJ618728	FJ618685	FJ618773
ST8	*A. gemina*	USA: New York	JF313136	*PP481937*	*PP342535*	*PP484606*	*PP501806*
ST9	*A. gemina*	USA: New York	JF313135	PP481938	PP342536	PP484607	PP501807
ST11	*A. gemina*	USA: West Virginia	*PP481738*	*PP481939*	*PP342537*	*PP484608*	*PP501808*
PB71.1	*A. cepistipes*	France	FJ618641	FJ618596	FJ618727	FJ618684	FJ618772
PE71.2	*A. gallica*	France	FJ618638	FJ618593	FJ618724	FJ618681	FJ618769
PVI85.43	*A. mellea*	USA: California	FJ618648	FJ618603	FJ618734	FJ618691	FJ618779
VI49.5	*A. mellea*	USA: Massachusetts	FJ618675	FJ618631	FJ618762	FJ618718	FJ618806
V48.5	*A. sinapina*	Canada	FJ618676	FJ618632	FJ618763	FJ618719	FJ618807
OHIO_2018PB-1	*Desarmillaria caespitosa*	USA: Ohio	MT232065	*PP481931*	MT238204	MN996977	*PP501800*
OOI-210	*D. caespitosa*	USA: Georgia	MT232068	MT225098	*PP342532*	MN996984	MN990679
PT84-12	*D. tabescens*	France	FJ618658	FJ618613	FJ618744	FJ618700	FJ618788
PT89.84	*D. tabescens*	Italy	FJ618674	FJ618630	FJ618761	FJ618717	FJ618805
519	*D. tabescens*	Czech Republic	MT221655	MT225095	MT163173	MN996980	MN990672
525	*D. tabescens*	Czech Republic	MT221657	MT225097	MT163177	*PP484599*	MN990676
MY84-94-1	*D. ectypa*	France	FJ618643	FJ618598	FJ618729	FJ618686	FJ618774
Lot2	*A. hinnulea*	Australia	FJ618663	FJ618618	FJ618749	FJ618705	FJ618793
Plim84.66	*A. limonea*	New Zealand	FJ618654	FJ618609	FJ618740	FJ618697	FJ618785
VM5.2	*A. luteobubalina*	Australia	FJ618666	FJ618622	FJ618753	FJ618709	FJ618797
PNZ87.54	*A. novae-zelandiae*	Papua New Guinea	FJ618650	FJ618605	FJ618736	FJ618693	FJ618781
3626	*A. pallidula*	Australia	FJ618665	FJ618621	FJ618752	FJ618708	FJ618796
PPg85-63	*A. puiggarii*	Mexico	FJ618636	FJ618591	FJ618722	FJ618679	FJ618767

[a]The *tef1, rpb2, act, gpd*, or 28S sequences from selected *Armillaria* isolates for this study are deposited in GenBank (italicized).
[b]*tef1* = translation elongation factor 1-alpha; *act* = actin; 28S = a portion of the ribosomal large subunit 28S rDNA; *gpd* = glyceraldehyde-3-phosphate dehydrogenase; *rpb2* = RNA polymerase II second largest subunit.
[c]Epitype-derived isolate (ex-epitype).

Table 2. List of *Armillaria* genomes used to build a whole genome phylogenetic tree.

Isolate	Species	Study	GenBank number
GN1	*Armillaria solidipes*	This study	JBLIQK000000000
28-4	*A. solidipes*	Ibarra Caballero et al. (2023)	GCA_022307675
ID001	*A. solidipes*	Ibarra Caballero et al. (2023)	GCA_022818035
gfArmOsto1.1	*A. ostoyae*	Not published	GCA_964034915
C18/9	*A. ostoyae*	Sipos et al. (2017)	GCA_902506015
FPL87.14	*A. borealis*	Sahu et al. (2023)	GCA_030435635
AB13-TR4-IP16	*A. borealis*	Akulova et al. (2020)	GCA_013427175
Ar21-2	*A. gallica*	Cai et al. (2023)	GCA_002307695
NIFoS 2319	*A. gallica*	Not published	GCA_038088205
YAFMHJ89	*A. sinapina*	Not published	GCA_040085025
YAFA0618	*A. calvescens*	Not published	GCA_043748625
B5	*A. cepistipes*	Sipos et al. (2017)	GCA_900157415
837-10	*A. altimonana*	Ibarra Caballero et al. (2023)	CGA_022818075
CMW6904	*A. nabsnona*	Sahu et al. (2023)	CGA_030407065
ELD017	*A. mellea*	Sahu et al. (2023)	GCA_030407055
MEX87	*A. mexicana*	This study	JBLJFM000000000

(*act*), and a portion of the ribosomal large subunit 28S rDNA (28S). Five PCR primer sets for each locus were used for PCR and sequencing: EF983F and EF2218R for *tef1*; bRPB2-6 F and bRPB2-7.1 R for *rpb2*; ACT-181 and Act-875 R for *act*; GPD10F and GPD522R for *gpd*; and LROR and LR5 for 28S (Antonín et al. 2021). Amplification reaction mixtures (total 25 µL) contained 20–40 ng of template DNA (or no DNA template for negative control), 2.5 µL 10× Standard *Taq* Reaction Buffer (New England BioLabs, Ipswich, Massachusetts), 0.5 µL 10 mM dNTPs (Roche Applied Science, Madison, Wisconsin), 1 µL each of 10 µM primer, and 0.125 µL (0.6 U) *Taq* DNA Polymerase (New England BioLabs). Amplifications were performed

using the following polymerase chain reaction (PCR) conditions: 94 C for 1 min, 35 cycles at 95 C for 30s, 55–58 C (depending on the primers used: *tef1*: 55 C, *rpb2*: 56 C, *act*: 57 C, *gpd*: 55 C, and 28S: 58 C) for 30s, and 72 C for 45s, and finally 72 C for 10 min. PCR products were electrophoresed in 1.5% agarose gels with 0.5× TBE buffer (45 mM Tris pH 8.3, 45 mM boric acid, 1 mM Na_2EDTA) and stained with GelRed (Biotium, Fremont, California). Bands were visualized using ultraviolet light (UV) light. PCR products were treated with ExoSAP-IT PCR Product Cleanup (Affymetrix, Santa Clara, California) following the manufacturer's protocol and sequenced at Eurofins (Louisville, Kentucky). The newly determined *tef1, rpb2, act, gpd*, or 28S sequences from selected *Armillaria* isolates for this study are deposited in GenBank (TABLE 1).

Genome sequencing of type specimen GN1.—The *A. solidipes* isolate GN1 was subcultured onto sterile, 0.45-µm-pore nylon filters (Merck Life Science, Bangalore, India), which were placed on modified *Armillaria* MEA (1.5% malt extract, 1.5% glucose, 0.5% peptone, 1.2% agar) and cultured for 3 weeks at 22 C. DNA was extracted using a SYNERGY 2.0 Plant DNA Extraction Kit (OPS Diagnostics, Lebanon, New Jersey) following manufacturer's protocol. DNA concentration was measured using the NanoDrop 2000 spectrophotometer. Illumina sequencing was performed at Psomagen (Rockville, Maryland).

Genome assembly was completed using SPAdes 4.0.0 with default parameters but including the "isolate" argument to improve the assembly quality. The assembly was corrected and scaffolded with RagTag 2.1.0 (Hall and Nisbet 2023), using the reference genome of *A. solidipes* (National Center for Biotechnology Information [NCBI] ASM2281803v1). Scaffolds smaller than 500 bp were removed. Metrics of the genome assembly were obtained using the "stats" command in SeqKit 2.9.0 (Shen et al. 2024).

Phylogenetics.—Three data sets (1, 2, and 3) were used to build phylogenies to examine phylogenetic support for the separation of *A. solidipes* (North America) from *A. ostoyae* (Eurasia). First, separate phylogenies for each gene region, and then a phylogeny for the combined five loci (data set 1) were generated to determine the support for the separation of *A. ostoyae* and *A. solidipes* at each locus. We then generated a *tef1* phylogeny based on 187 sequences (including 11 sequences from data set 1) of *A. solidipes* and *A. ostoyae* deposited in GenBank (data set 2). Third, we compared the phylogenetic relationship of *A. solidipes* and *A. ostoyae* using the whole genome sequence of GN1 and other *Armillaria* genomes (data set 3).

Phylogenies of loci

Phylogenies were created in Geneious 9.0.5 (https://www.geneious.com) using both maximum likelihood (ML) in PhyML (Guindon et al. 2010) and Bayesian inference (BI) in MrBayes 3.2 (Ronquist et al. 2012) methods. ML phylogenies were run with 1000 bootstraps (BS) to assess clade support. For each locus, parameter settings for BI were selected by determining the best-fit nucleotide substitution model using IQ-TREE (Minh et al. 2020). Markov chain Monte Carlo (MCMC) with four chains each of length 1 100 000 was run, which generated 4402 to 11 002 trees, depending on the locus. The first 20% were discarded as burn-in, and posterior probability values were used to assess the support for each node. Visual inspection of trace plots was performed to ensure convergence of chains in BI, and the effective sample size for each analysis was >497. A combined-locus (data set 1) Bayesian phylogeny was built using the software BEAUti2 and BEAST 2.6.0 (Drummond et al. 2012). BEAUti2 was used to format the XML file used for analyses implemented in BEAST. Models of evolution were set for each individual locus (SUPPLEMENTARY TABLE 1), but a combined phylogeny was the output in BEAST. Four independent runs with 10 million generations were run and sampled every 1000 generations. Tracer 1.7 was used to assess the effective sampling size to ensure appropriate parameter convergency. TreeAnnotator 1.10 was used to annotate and summarize the combined maximum clade credibility phylogeny after discarding 20% burn-in. FigTree 1.4.4 was used to visualize the resulting trees and the posterior probably values.

Translation elongation factor 1-alpha (tef1) *phylogeny*

Data set 2 was compiled that included sequences from the original isolates used in data set 1 along with an additional 176 sequences from globally distributed *A. solidipes, A. ostoyae*, and other *Armillaria* spp. downloaded from GenBank (see SUPPLEMENTARY FIG. 5). Again, the ML phylogeny was run with 1000 BS, and parameter settings for BI were selected by determining the best-fit nucleotide substitution model using IQ-TREE. Markov chain Monte Carlo (MCMC) with four chains each of length 5 000 000 was run, which generated 10 002 trees. The first 20% were discarded as burn-in, and posterior probability values were used to assess the support for each node.

Whole genome phylogeny

The ML phylogeny was generated using whole genome sequences of *Armillaria* spp., including a genome sequence of GN1 (data set 3; TABLE 2), using kSNP4.1 (Hall and Nisbet 2023) with 31 as optimum value of k as determined by the program and 100 bootstraps to assess node support.

RESULTS

***Genome assembly of* A. solidipes *isolate GN1.*—**A total of 3 870 881 074 bases in 25 634 974 paired-end reads were obtained from genomic sequencing of *A. solidipes* isolate GN1. Quality of the reads was accessed using FastQC 0.11.4. No trimming was needed given the high quality of all reads. The assembled genome of *A. solidipes* isolate GN1 (JBLIQK000000000) consisted of 7691 scaffolds, for a total of 56.5 Mb. The N50 value was 1 954 351, and the GC content was 45.72%. No contamination with DNA sequences from any other organism was detected after running BLASTn of the scaffolds against the NCBI Nucleotide database.

***Phylogenetic analyses.*—**Phylogenetic analyses of *tef1* sequences showed that *A. solidipes* [from North America (NA)] clustered within a well-separated clade distinct from the clade containing *A. ostoyae* (from Eurasia including Germany, Italy, and South Korea) (FIG. 2). Unlike the *tef1* phylogenies, the phylogeny of *rpb2* revealed that sequences from all but one *A. solidipes* isolate (ST1) were separated from *A. ostoyae*, but both *A. solidipes* and *A. ostoyae* were clearly separated from other closely related species (e.g., *A. gemina, A. borealis* Marxm. & Korhonen) (SUPPLEMENTARY FIG. 1). The *act* phylogeny did not clearly resolve sequences of all *A. solidipes* and *A. ostoyae* isolates; however, *A. gemina* sequences were clearly separated from all sequences from both *A. solidipes* and *A. ostoyae* (SUPPLEMENTARY FIG. 2). Phylogenic signals from *gpd* separated only three of the eight *A. solidipes* isolates, with sequences of other *A. solidipes* isolates intermixed with sequences from *A. ostoyae* isolates and an *A. borealis* isolate and *A. gemina* isolates were separated into two distinct clades (SUPPLEMENTARY FIG. 3). The 28S phylogeny was the least informative of the loci analyzed,

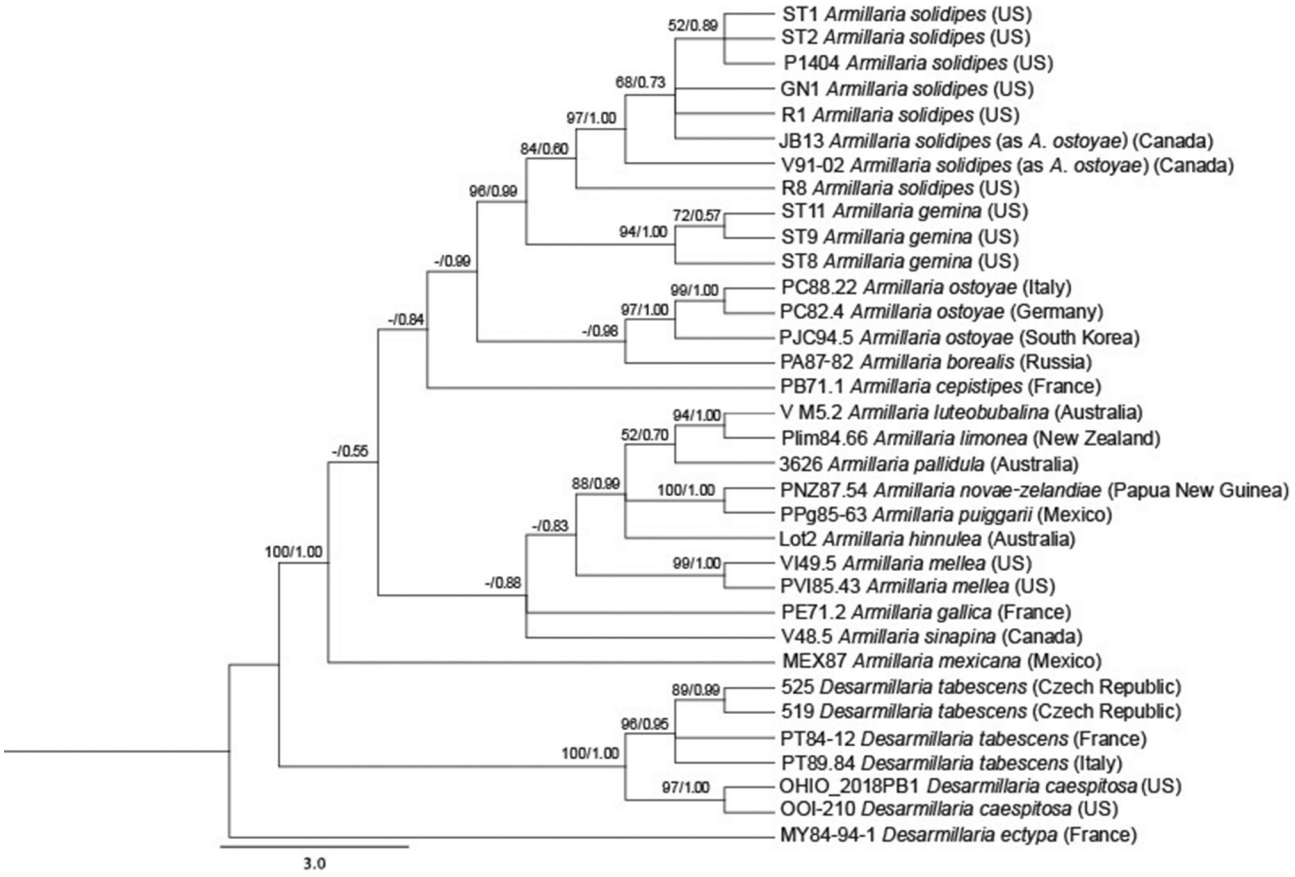

Figure 2. Maximum likelihood phylogeny of the translation elongation factor 1-alpha (*tef1*), with well-supported nodes (BS/PP) separating sequences of *Armillaria solidipes* and *A. ostoyae*. Isolates of *A. solidipes, A. ostoyae*, and other *Armillaria/Desarmillaria* are described in TABLE 1.

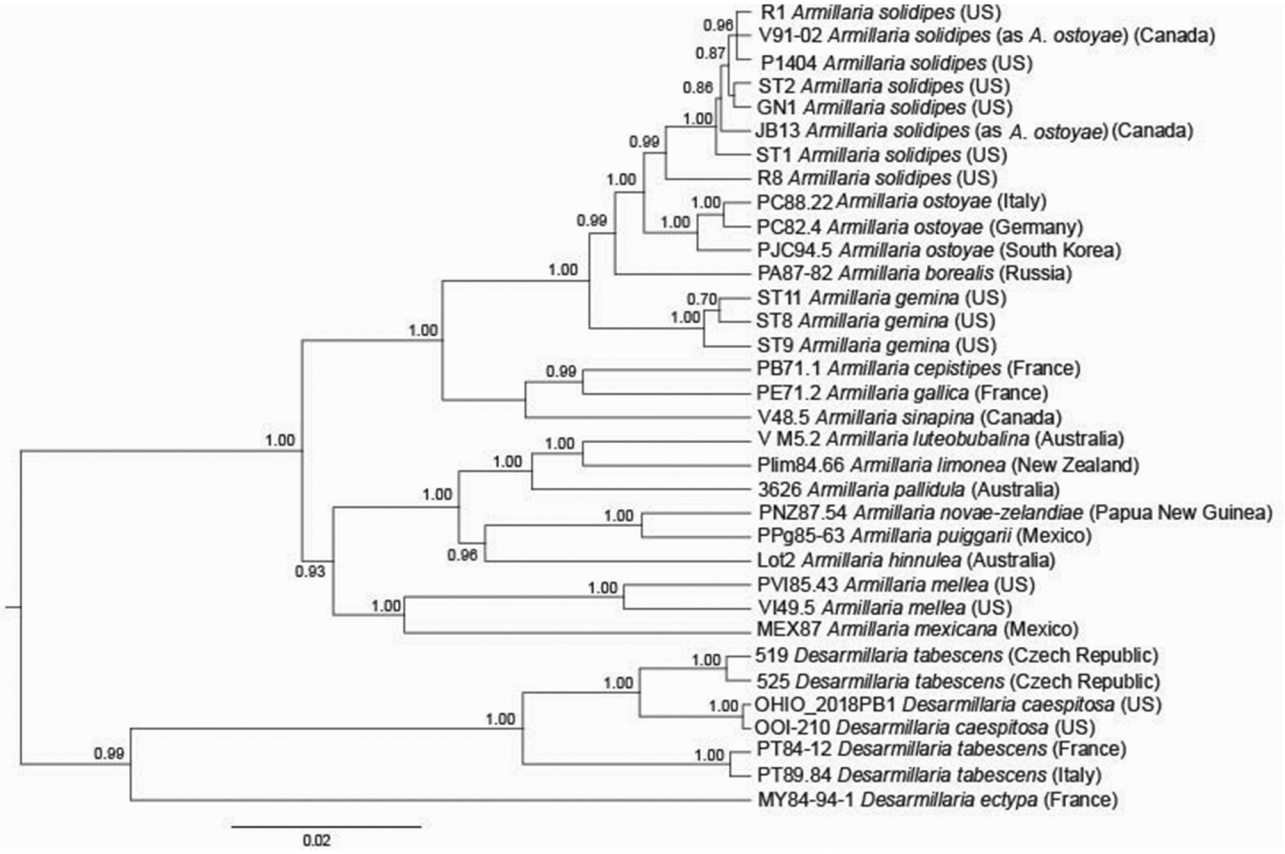

Figure 3. Bayesian inference phylogenetic tree of concatenated loci (*tef1, rpb2, gpd, act*, and 28S) of sequences from *Armillaria*/*Desarmillaria* species isolates, with well-supported nodes (BS/PP) separating sequences of *Armillaria solidipes* and *A. ostoyae*. Isolates of *A. solidipes, A. ostoyae*, and other *Armillaria*/*Desarmillaria* are described in TABLE 1. *tef1* = translation elongation factor 1-alpha; *act* = actin; 28S = a portion of the ribosomal large subunit 28S rDNA; *gpd* = glyceraldehyde-3-phosphate dehydrogenase; *rpb2* = RNA polymerase II second largest subunit.

with little phylogenetic signals to distinguish *A. solidipes* and *A. ostoyae* within clusters containing multiple *Armillaria* spp.; however, *A. gemina* was comprised within a distinct clade (SUPPLEMENTARY FIG. 4).

The larger phylogeny of the *tef1* region, with additional *A. solidipes* and *A. ostoyae* sequences (data set 2), showed a clear and well-supported distinction of isolates collected from North America from those collected from Eurasia (SUPPLEMENTARY FIG. 5). The phylogeny also supported distinct clades within each species, highlighting previously undescribed genetic structure within *A. solidipes* and *A. ostoyae*. The phylogenetic tree based on five loci strongly supported the distinction among *A. solidipes*, *A. ostoyae*, and *A. gemina* (FIG. 3).

The whole genome phylogeny (data set 3) concurred with *tef1* and combined-locus phylogenetic trees (FIG. 4), all of which provided strong support for the separation between *A. ostoyae* from Eurasia and *A. solidipes* from North America. Furthermore, the whole genome phylogeny demonstrates that the separate *A. ostoyae* and *A. solidipes* clades are also clearly distinct from other *Armillaria* species for which whole genome sequences are available.

TAXONOMY

Armillaria solidipes Peck, Bulletin of the Torrey Botanical Club 27(12): 611, 1900.

= *Armillariella solidipes* (Peck) T.J. Baroni, Mycologia 73(1):186. 1981.

Holotype: USA. COLORADO: Gunnison County, Mill Creek, 2 Sep 1899, *E. Bartholomew 2690* (FH).

Epitype: USA. COLORADO: Gunnison, Mill Creek Trail, 38.69379N, 107.07432W, 29 Aug 2018, *Suzanne B. Marchetti & James J. Worrall* (BRNM 847568, ATCC 2024-TSDA-00053, MBT 10025258).

Description of the epitype (macroscopic description by J.J. Worrall): Pileus 20–50 mm broad, convex, finely striate at margin, buff brown (±6C–D6), overlaid with darker fine scales, ochraceous near the apex. Lamellae close, attached, slightly decurrent, cream-colored. Stipe

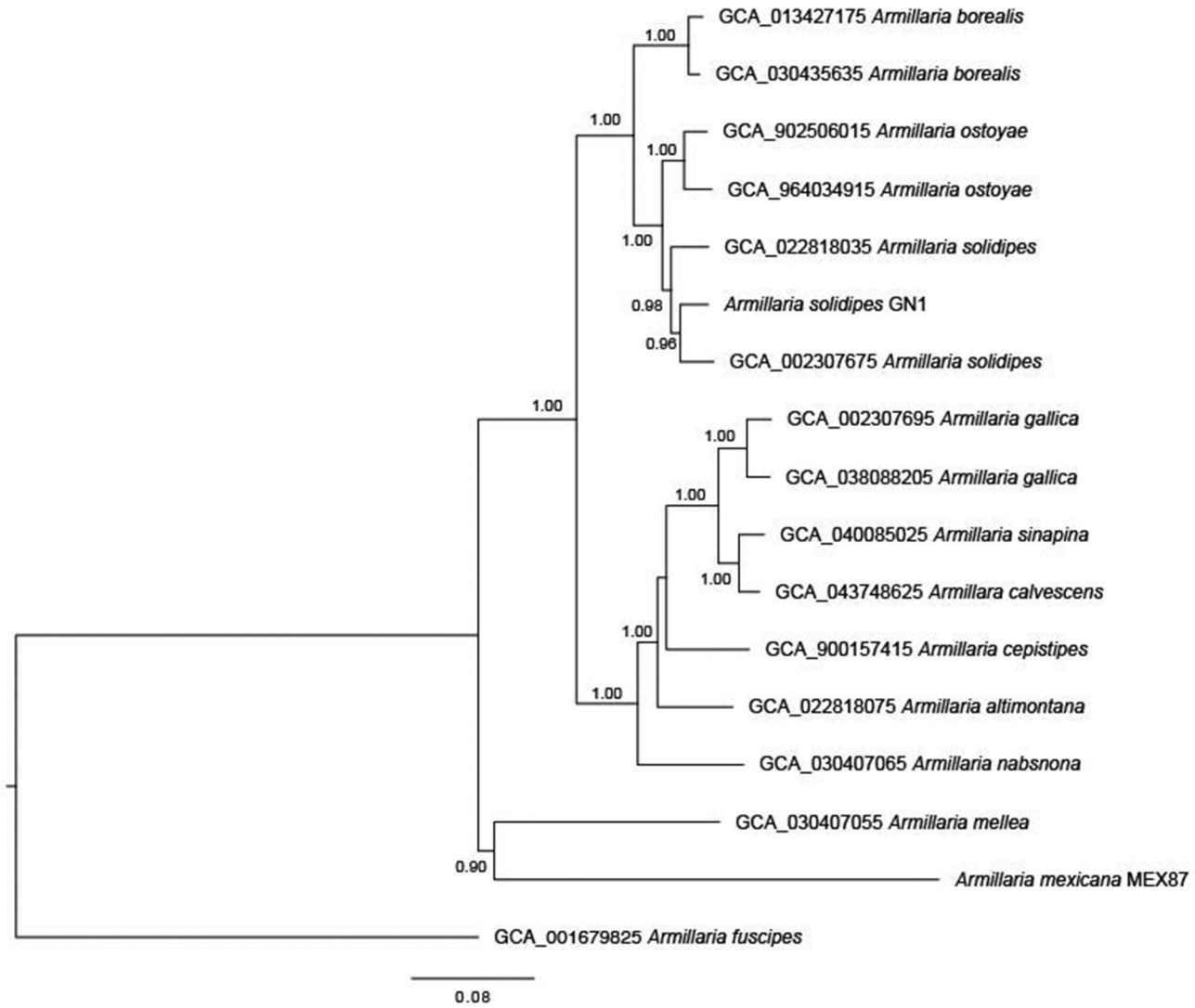

Figure 4. Maximum likelihood phylogeny of genome sequences of *Armillaria* species. Isolates of *A. solidipes, A. ostoyae*, and other *Armillaria* are described in TABLE 2.

50–70 mm long, broadening at base, tan (±6C5–6D5) with white zones and brown flecks, yellow scales at the base. Annulus white with yellow edges and brown flecks; when partial veil is intact, the attachment is fragile, wispy, but looks membranaceous as a ring. Overall darkening with age to a more uniform umber brown.

Basidiospores [30/1/1] (7.0–)7.5–9.0(–11) × (5.0–)5.3–6.5(–7.0) µm, average 8.17 × 5.82 µm, E = (1.15–)1.25–1.58(–1.64), Q = 1.41, ellipsoid, broadly ellipsoid, broadly subamygdaliform, thin- to slightly thick-walled, non-dextrinoid. Basidia [15/1/1] 31–48 × 7.0–10 µm, 4-spored, clavate, sometimes with clamp connections; crassobasidia present (walls up to 1.0 µm thick). Basidioles 14–40 × 4.0–10 µm, clavate, cylindrical, subfusoid; crassobasidioles present. Cheilocystidia [20/1/1] 18–41 × 6.0–11 µm, variable in shape, fusoid, subcylindrical, clavate, utriform, mostly irregular and with irregular rostrum, less frequently simple, thin- or ±slightly thick-walled, sometimes with medallion-type clamp connections. Trama hyphae cylindrical, thin-walled, non-dextrinoid, 2.0–8.0 µm wide. Pileipellis a cutis composed of cylindrical to (sub)fusoid, thin- to slightly thick-walled, colorless to pale brownish, clamp-less, 3.0–10 µm wide hyphae; upper part of pileipellis of similar chains of cells like scales, but ±colorless and slightly smaller. Pileus scales composed of chains of ellipsoid, cylindrical, rarely subfusoid, slightly thick-walled (walls up to 1.0 µm), brownish to brown in KOH, 9.0–25 µm wide hyphae; terminal cells 23–95 × 9.0–20 µm, conical, conical-fusoid, less frequently sub-cylindrical. Annulus hyphae and velar remnants made up of chains of up to 150 × 8.0–25 µm, cylindrical, ellipsoid, rarely broadly ellipsoid, thin- to slightly

thick-walled, colored or slightly brownish cells; terminal cells 39–95 × 8.0–22 µm, ellipsoid, subfusoid, clavate, subulate, thin- to slightly thick-walled, colorless to brown. Stipitipellis of cylindrical, slightly thick-walled, clampless, 3.0–6.0 µm wide hyphae; terminal cells adpressed to (sub)erect, cylindrical, narrowly clavate, narrowly fusoid, obtuse, 4.0–8.0 µm wide.

Ecology: Fruiting on buried root of living *Picea engelmannii* Parry ex Engelm.

DISCUSSION

Both *A. solidipes* and *A. ostoya*e are well-known, widespread, and destructive pathogens that cause Armillaria root disease of diverse conifers and hardwoods. However, our results here show that *A. solidipes* is found in North America, whereas *A. ostoyae* is found in diverse forests of Eurasia. Our data highlight morphological and molecular differences between *A. solidipes* and *A. ostoyae*, and the specimen BRNM 847568 from Colorado, USA, is designated as the epitype for *A. solidipes*.

The morphological differences between *A. solidipes* and *A. ostoyae* are discussed below. *Armillaria solidipes* is characterized by a buff to brown pileus with fine brown scales, a broadening base with yellow scales, a tan-colored stipe with white zones and brown dots, a white ring with yellow to brown edge, moderately large basidiospores, variable, fusoid, subcylindrical, clavate, utriform, mostly irregular and irregularly rostrate cheilocystidia, and pileus scales composed of chains of ellipsoid, cylindrical, rarely subfusoid hyphae with 23–95 × 9.0–20 µm, conical, conical-fusoid, less frequently subcylindrical terminal cells. The macroscopic characters agree with those described by Peck (1900) except for shorter stipe, and microscopic description agrees well with the type studies by Burdsall and Volk (2008) and Baroni (1981) except for slightly broader basidiospores, (8–)8.5–11.5 × (5.5–)6.0–7.5 µm, by Baroni (1981).

Armillaria ostoyae differs by a darker, brown-ochraceous to reddish or violaceous brown pileus with close dark brown to black-brown, more or less pyramidal scales, reddish to almost violaceous lamellae in mature specimens, a stipe with more distinct velar remnants, smaller cheilocystidia—approximately 12–28 × 4.5–8.5–11 µm according to Romagnesi (1970), but larger, 16–35 × 4.5–11 µm, according to Antonín (unpubl. studies)—which are cylindrical, subclavate, ellipsoid, regular or irregular, and only rarely with a short rostrum and longer, (15–)25–140 × 5.0–25 µm, pileipellis terminal cells (Antonín unpubl.; Romagnesi 1970, 1973). *Armillaria borealis* is macromorphologically rather similar. It differs by a pileus covered with not close, small, concolorous to slightly darker scales, a stipe with yellowish to pale brown scales, and slightly different basidiospores, 7–8.5 × 4.5–5.5 µm (Kibby 2013), (6–)7.2–9.6(–12) µm long (Marxmüller 1986), but 7.0–12 × 6.0–8.5 µm according to Antonín (unpubl. studies). *Armillaria sinapina* Bérubé & Dessur. especially differs by a yellow-colored annulus without darker edge and/or yellow remnants on the stipe, distinctly broader, 8.2–10 × 5.9–8 µm, basidiospores, and shorter, 32–68 × 4–14 µm, terminal pileipellis cells (Bérubé and Dessureault 1988); moreover, the authors have not described any cheilocystidia. *Armillaria gemina* is macro- and micromorphologically also very close to *A. solidipes*. In fact, it differs only by a mostly larger pileus and smaller cells of the pileus scales (22–58 × 5–18 µm); it was collected only on broadleaved trees (Bérubé and Dessureault 1989).

According to Klopfenstein et al. (2017) and Coetzee et al. (2018), *A. solidipes* belongs, together with *A. ostoyae, A. gemina, A. borealis*, and two collections identified as *A. cepistipes* Velen., to the Solidipes/Ostoyae superclade. Liang et al. (2021) also included it to the Solidipes/Ostoyae superclade, which is divided into at least two unnamed lineages. Our whole genome phylogenetic analyses concur with these results, yet we also show that *A. solidipes* isolates form a well-supported and distinct clade from *A. ostoyae*.

Previous phylogenetic analyses and the analysis herein have determined that *tef1* sequences are a reliable means to distinguish *A. solidipes* and *A. ostoyae* (e.g., Guo et al. 2016; Klopfenstein et al. 2017; Liang et al. 2021), whereas other housekeeping loci contribute limited phylogenetic signals for distinguishing *A. solidipes*. *tef1* sequences have been used to identify *A. solidipes* associated with diverse hosts and geographic regions in the USA (e.g., Arizona, Colorado, Idaho, Massachusetts, Minnesota, Montana, New Hampshire, New Mexico, North Carolina, Oregon, Utah, Washington, and Wyoming, among others) and Canada (e.g., British Columbia and Newfoundland, among others) (Kim et al. 2023, 2021, 2022; Klopfenstein et al. 2017; Liang et al. 2021; Ross-Davis et al. 2012). To accurately delineate *A. solidipes* from its closely related sister taxon, *A. gemina*, particularly in regions where their distributions may overlap (e.g., the eastern Appalachian Mountains), we recommend sequencing an additional gene region, such as *rpb2* or *act*, in addition to *tef1*.

Based on *tef1*-based identification, it is especially noteworthy that *A. solidipes* has not been previously reported in Eurasia, nor has *A. ostoyae* been previously reported in North America. For this reason, it seems likely that all previous reports of *A. ostoyae* in North America should currently be considered to be *A. solidipes* (and all previous reports of *A. solidipes* in Eurasia

should likely be considered to be *A. ostoyae*). Our ex-epitype *A. solidipes* (isolate GN1) is phylogenetically clustered with other *A. solidipes* isolates from North America, and it is clearly separated from *A. ostoyae* based on *tef1* locus and whole genome analyses. Previous studies using whole genome phylogenetic analyses also strongly supported that these two *Armillaria* spp. are separate but closely related species (Ibarra Caballero et al. 2023; Sipos et al. 2017). Ibarra Caballero et al. (2023) showed that *A. ostoyae* isolate (C18/9 from Switzerland) is clearly separated from two North American *A. solidipes* (ID001 from Idaho and 28-4 from Vermont) using the whole genome phylogenetic analysis.

Our phylogenetic results from the *tef1* sequences of *A. solidipes* and *A. ostoyae* downloaded from GenBank show that all isolates from Eurasia are *A. ostoyae* and all of those from North America are *A. solidipes*. Thus, it is critical to recognize that *A. solidipes* represents an invasive species threat to geographic areas with suitable climate in Eurasia (and elsewhere where it does not currently exist) and that *A. ostoyae* represents an invasive species threat to areas with suitable climate in North America (and elsewhere where it does not currently exist). Furthermore, the apparent interfertility of *A. solidipes* and *A. ostoyae* elevates the invasive threats associated with these species due to the unknown consequences of interspecific hybridization and introgression of these species. In addition, damage caused by *A. solidipes* and *A. ostoyae* is predicted to increase under future climate change due to maladaptation and/or stress of host trees (e.g., Kim et al. 2021; La Porta et al. 2008); however, it is unknown whether these species will behave differently under new climates. For these reasons, it is critical that *A. solidipes* and *A. ostoyae* be recognized as distinct species for regulatory, research, inventory, ecological, and forest management purposes.

ACKNOWLEDGMENTS

This study was partially supported by the employees of the United States Department of Agriculture (USDA) Forest Service, R&D, Rocky Mountain Research Station and Pacific Northwest Research Station. The findings and conclusions in this publication are those of the authors and should not be construed to represent any official USDA or U.S. Government determination or policy.

DISCLOSURE STATEMENT

No potential conflict of interest was reported by the author(s).

DATA AVAILABILITY STATEMENT

The sequences from selected *Armillaria* isolates used in this study have been deposited in GenBank. Supplemental sequence alignment data for this article are available online at https://doi.org/10.6084/m9.figshare.29270894.v1.

FUNDING

This project has been supported by USDA Forest Service (FS), State, Private, and Tribal Forestry, Forest Health Protection Special Technology and Development Program [STDP R5-2023-01 and STDP R2-2023-01], and FS Research & Development Infrastructure Investment and Jobs Act Research Project ERR09. Studies by V. Antonín were facilitated by support to the Moravian Museum from the Ministry of Culture of the Czech Republic as a part of its long-term conceptual development program for research institutions [DKRVO, ref. MK000094862].

ORCID

Vladimír Antonín http://orcid.org/0000-0002-6000-7285
Ada J. Fitz Axen http://orcid.org/0009-0007-1245-1561
Jorge R. Ibarra Caballero http://orcid.org/0000-0001-6007-5168
James J. Worrall http://orcid.org/0000-0001-7504-5201
Jane E. Stewart http://orcid.org/0000-0001-9496-6540
Ned B. Klopfenstein http://orcid.org/0000-0002-9776-3973
Mee-Sook Kim http://orcid.org/0000-0001-7073-6708

LITERATURE CITED

Akulova VS, Sharov VV, Aksyonova AI, Putintseva YA, Oreshkova NV, Feranchuk SI, Kuzmin DA, Pavlov IN, Litovka YA, Krutovsky KV. 2020. De novo sequencing, assembly and functional annotation of *Armillaria borealis* genome. BMC Genomics. 21:534. doi:10.1186/s12864-020-06964-6.

Anderson JB, Korhonen K, Ullrich RC. 1980. Relationships between European and North American biological species of *Armillaria mellea*. Exp Mycol. 4:87–95. doi:10.1016/0147-5975(80)90053-5.

Anderson JB, Ullrich RC. 1979. Biological species of *Armillaria mellea* in North America. Mycologia. 71:402–414. doi:10.1080/00275514.1979.12021018.

Antonín V, Stewart JE, Medel Ortiz R, Kim M-S, Bonello PE, Tomšovský M, Klopfenstein NB. 2021. *Desarmillaria caespitosa*, a North American vicariant of *D. tabescens*. Mycologia. 113:776–790. doi:10.1080/00275514.2021.1890969.

Baroni TJ. 1981. Collections in the Farlow Herbarium: new species of *Melanophyllum* and *Gastrocybe*, type studies on *Armillaria* and *Stropharia*. Mycologia. 73:186–197. doi:10.1080/00275514.1981.12021331.

Bérubé JA, Dessureault M. 1988. Morphological characterization of *Armillaria ostoyae* and *Armillaria sinapina* sp.nov. Can J Bot. 66:2027–2034. doi:10.1139/b88-277.

Bérubé JA, Dessureault M. 1989. Morphological studies of the *Armillaria mellea* complex: two new species, *A. gemina* and *A.*

calvescens. Mycologia. 81:216–225. doi:10.1080/00275514.1989.12025650.
Burdsall HH Jr, Volk TJ. 1993. The state of taxonomy of the genus *Armillaria*. McIlvainea. 11:1–12.
Burdsall HH Jr, Volk TJ. 2008. *Armillaria solidipes*, an older name for the fungus called *Armillaria ostoyae*. North Am Fungi. 3:261–267. doi:10.2509/naf2008.003.00717.
Cai J, Muhammad I, Chen B, Xu P, Li Y, Xu H, Li K. 2023. Whole genome sequencing and analysis of *Armillaria gallica* Jzi34 symbiotic with *Gastrodia elata*. BMC Genomics. 24:275. doi:10.1186/s12864-023-09384-4.
Coetzee MPA, Wingfield BD, Wingfield MJ. 2018. Armillaria root-rot pathogens: species boundaries and global distribution. Pathogens. 7:83. doi:10.3390/pathogens7040083.
Drummond AJ, Suchard MA, Xie D, Rambaut A. 2012. Bayesian phylogenetic with BEAUti and the BEAST 1.7. Mol Biol Evol. 29:1969–1973. doi:10.1093/molbev/mss075.
Guindon S, Dufayard J-F, Lefort V, Anisimova M, Hordijk W, Gascuel O. 2010. New algorithms and methods to estimate maximum-likelihood phylogenies: assessing the performance of PhyML 3.0. Syst Biol. 59:307–321. doi:10.1093/sysbio/syq010.
Guo T, Wang HC, Xue WQ, Zhao J, Yang ZL. 2016. Phylogenetic analyses of *Armillaria* reveal at least 15 phylogenetic lineages in China, seven of which are associated with cultivated *Gastrodia elata*. PLOS ONE. 11:e0154794. doi:10.1371/journal.pone.0154794.
Hall BG, Nisbet J. 2023. Building phylogenetic trees from genome sequences with kSNP4. Mol Biol Evol. 40: msad235. doi:10.1093/molbev/msad235.
Heinzelmann R, Dutech C, Tsykun T, Labbé F, Soularue J-P, Prospero S. 2019. Latest advances and future perspectives in *Armillaria* research. Can J Plant Pathol. 41:1–23. doi:10.1080/07060661.2018.15558284.
Herink J. 1973. Taxonomie václavky obecné – *Armillaria mellea* (Vahl ex Fr.) Kumm. In: Hašek J, editor. Sympozium o václavce obecné: *Armillaria mellea* (Vahl ex Fr.) Kumm. September 28–29, 1972. Brno (Czechoslovakia): Vysoká Škola Zemědělská v Brně. p. 21–48.
Hintikka V. 1973. A note on the polarity of *Armillariella mellea*. Karstenia. 13:32–39. doi:10.29203/ka.1973.80.
Ibarra Caballero JR, Lalande BM, Hanna JW, Klopfenstein NB, Kim M-S, Stewart JE. 2023. Genomic comparisons of two *Armillaria* species with different ecological behaviors and their associated soil microbial communities. Microb Ecol. 85:708–729. doi:10.1007/s00248-022-01989-8.
Kibby G. 2013. Fungal portraits no. 53. *Armillaria borealis*. Field Mycol. 14:3–4. doi:10.1016/j.fldmyc.2012.12.003.
Kim M-S, Blaedow RA, McKeever KM, Olatinwo RO, Klopfenstein NB. 2023. First report of the Armillaria root disease pathogen, *Armillaria solidipes*, on black oak (*Quercus velutina*) in North Carolina, U.S.A. Plant Dis. 107:2261. doi:10.1094/PDIS-11-22-2689-PDN.
Kim M-S, Hanna JW, Stewart JE, Warwell MV, McDonald GI, Klopfenstein NB. 2021. Predicting present and future suitable climate spaces (potential distributions) of and Armillaria root disease pathogen (*Armillaria solidipes*) and its host, Douglas-fir (*Pseudotsuga menziesii*), under changing climates. Front For Glob Change. 4:740994. doi:10.3389/ffgc.2021.740994.
Kim M-S, Heinzelmann R, Labbé F, Ota Y, Elías-Román RD, Pildain MB, Stewart JE, Woodward S, Klopfenstein NB. 2022. Armillaria root diseases of diverse trees in widespread global regions, chapter 20. In: Asiegbu FO, Kovalchuk A, editors. Forest microbiology forest tree health. Vol. 2. London: Academic Press (Elsevier); p. 361–378. doi:10.1016/B978-0-323-85042-1.00004-5.
Klopfenstein NB, Stewart JE, Ota Y, Hanna JW, Richardson BA, Ross-Davis AL, Elías-Román RD, Korhonen K, Keča N, Iturritxa E, et al. 2017. Insights into the phylogeny of Northern Hemisphere *Armillaria*: neighbor-net and Bayesian analyses of translation elongation factor 1-α gene sequences. Mycologia. 109:75–91. doi:10.1080/00275514.2017.1286572.
Koch RA, Wilson AW, Séné O, Henkel TW, Aime MC. 2017. Resolved phylogeny and biogeography of the root pathogen *Armillaria* and its gasteroid relative. Guyanagaster BMC Evol Biol. 17:33. doi:10.1186/s12862-017-0877-3.
Korhonen K. 1978. Interfertility and clonal size in the *Armillariella mellea* complex. Karstenia. 18:31–42. doi:10.29203/ka.1978.135.
Kornerup A, Wanscher JH. 1983. Methuen handbook of colour. 3rd ed. London (UK): Eyre Methuen.
La Porta N, Capretti P, Thomsen IM, Kasanen R, Hietala AM, Von Weissenberg K. 2008. Forest pathogens with higher damage potential due to climate change in Europe. Can J Plant Pathol. 30:77–195. doi:10.1080/07060661.2008.10540534.
Liang J, Pecorato L, Cai L, Yuan P, Zhao P, Tsui CKM, Zhang Z. 2021. Phylogenetic relationships, speciation, and origin of *Armillaria* in the Northern Hemisphere: a lesson based on rRNA and elongation factor 1-alpha. J Fungi. 7:1088. doi:10.3390/jof7121088.
Marxmüller H. 1986. *Armillaria borealis* Marxmüller et Korhonen. Bulletin de la Société Mycologique France. 102 (3):244.
Marxmüller H. 1992. Some notes on the taxonomy and nomenclature of five European *Armillaria* species. Mycotaxon. 44:267–274.
Minh BQ, Schmidt HA, Chernomor O, Schrempf D, Woodhams MD, von Haeseler A, Lanfear R. 2020. Iq-tree 2: new models and efficient methods for phylogenetic inference in the genomic era. Mol Biol Evol. 37:1530–1534. doi:10.1093/molbev/msaa015.
Peck CH. 1900. New species of fungi. Bull Torrey Botanical Club. 27:609–613.
Redhead SA, Bérubé J, Cleary MR, Holdenrieder O, Hunt RS, Korhonen K, Marxmüller H, Morrison DJ. 2011. (2033) Proposal to conserve *Armillariella ostoyae* (*Armillaria ostoyae*) against *Agaricus obscurus, Agaricus occultans*, and *Armillaria solidipes* (*Basidiomycota*). Taxon. 60:1770–1771. doi:10.1002/tax.606023.
Romagnesi H. 1970. Observations sur les *Armillariella* (i). Bulletin Trimestriel de la Société Mycologique France. 86:257–265.
Romagnesi H. 1973. Observations sur les *Armillariella* (ii). Bulletin de la Société Mycologique France. 89:195–206.
Ronquist F, Teslenko M, van der Mark P, Ayres DL, Darling A, Hohna S, Larget B, Liu L, Suchard MA, Huelsenbeck JP. 2012. MrBayes 3.2: efficient Bayesian phylogenetic inference and model choice across a large model space. Syst Biol. 61:539–542. doi:10.1093/sysbio/sys029.
Ross-Davis AL, Hanna JW, Kim M-S, Klopfenstein NB. 2012. Advances toward DNA-based identification and phylogeny of

North American *Armillaria* species using elongation factor-1 alpha gene. Mycoscience. 53:161–165. doi:10.1007/S10267-011-0148-X.

Sahu N, Indic B, Wong-Bajracharya J, Merényi Z, Ke HM, Ahrendt S, Monk TL, Kocsubé S, Drula E, Lipzen A, et al. 2023. Vertical and horizontal gene transfer shaped plant colonization and biomass degradation in the fungal genus *Armillaria*. Nat Microbiol. 8:1668–1681. doi:10.1038/s41564-023-01448-1.

Shen W, Sipos B, Zhao L. 2024. Seqkit2: a Swiss army knife for sequence and alignment processing. iMeta. 3:e191. doi:10.1002/imt2.191.

Sipos G, Prasanna AN, Walter MC, O'Connor E, Bálint B, Krizsán K, Kiss B, Hess J, Varga T, Slot J, et al. 2017. Genome expansion and lineage-specific genetic innovations in the forest pathogenic fungi *Armillaria*. Nat Ecol Evol. 1:1931–1941. doi:10.1038/s41559-017-0347-8.

Thiers B. continuously updated. Index Herbariorum: a global directory of public herbaria and associated staff. New York Botanical Garden's virtual herbarium; [accessed 2025 Jan 30]. http://sweetgum.nybg.org/ih/.

Wilson KL. 2017. Report of the general committee: 18. Taxon. 66:742–744. doi:10.1002/tax.13151.